Science Advances
AAAS

advances.sciencemag.org/cgi/content/full/4/7/eaas9660/DC1

Supplementary Materials for

Hidden CDW states and insulator-to-metal transition after a pulsed femtosecond laser excitation in layered chalcogenide 1T-$TaS_{2-x}Se_x$

Kai Sun, Shuaishuai Sun, Chunhui Zhu, Huanfang Tian, Huaixin Yang, Jianqi Li*

*Corresponding author. Email: ljq@aphy.iphy.ac.cn

Published 20 July 2018, *Sci. Adv.* **4**, eaas9660 (2018)
DOI: 10.1126/sciadv.aas9660

This PDF file includes:

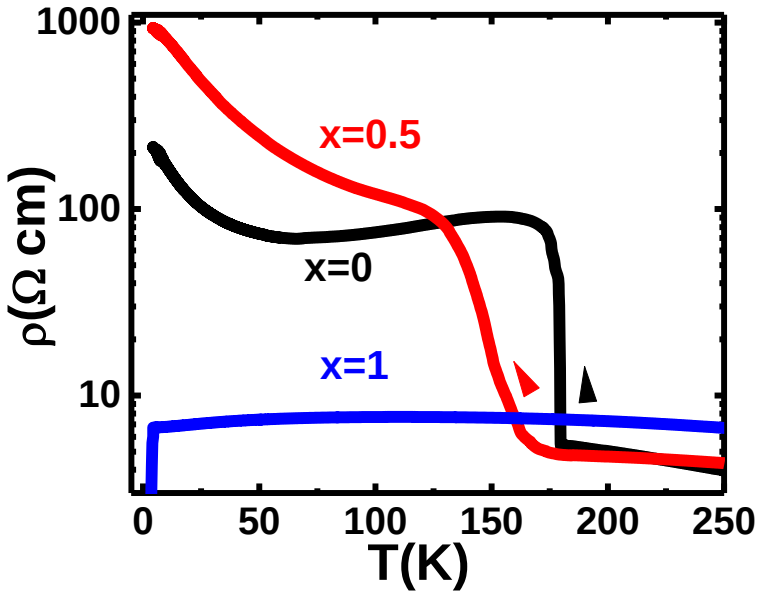

Fig. S1. Resistivity curves for the samples used in this study. Temperature dependence of resistivities for 1T-$TaS_{2-x}Se_x$ single crystal with x = 0, 0.5, and 1, indicating the transitions from NCCDW to CCDW by arrows.

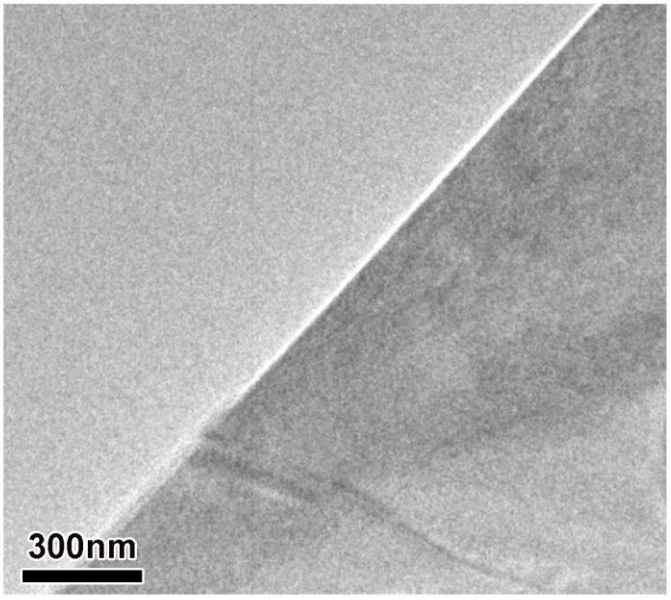

Fig. S2. TEM bright-field image of 1T-TaS_2. Bright-field images obtained along [001] zone-axis direction at 10 K for x = 0 sample. A remarkable structure defect indicates the observed area.

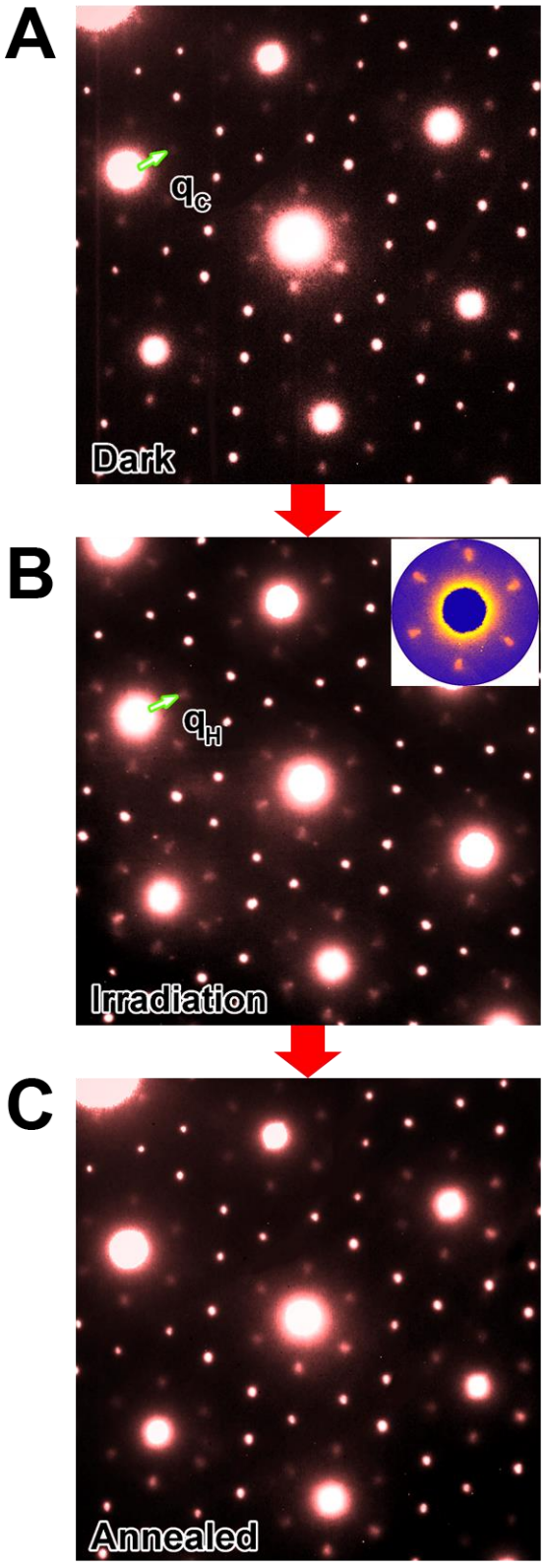

Fig. S3. In situ observation for the electron diffraction patterns of 1T-$TaS_{1.5}Se_{0.5}$. (Color online) Electron diffraction along the [001] zone-axis direction for x = 0.5 sample at 10 K under (**A)** dark (CCDW), (**B)** irradiation, and (**C)** after annealed, showing the space-anomaly H-CDW state microstructure in terms of clear satellite

spots splitting, the inset shows the enlarged diffraction spot. An annealing process is also able to drive the diffraction pattern of space-anomaly H-CDW state back to CCDW (Mott ground state), which follows the thermal erasure behavior of x=0 sample. Whereas, the situation remains unchanged when increasing the fluence up to 5 mJ/cm^2 instead of an obvious orientation anomaly in H-CDW state existing in the x=0 sample.

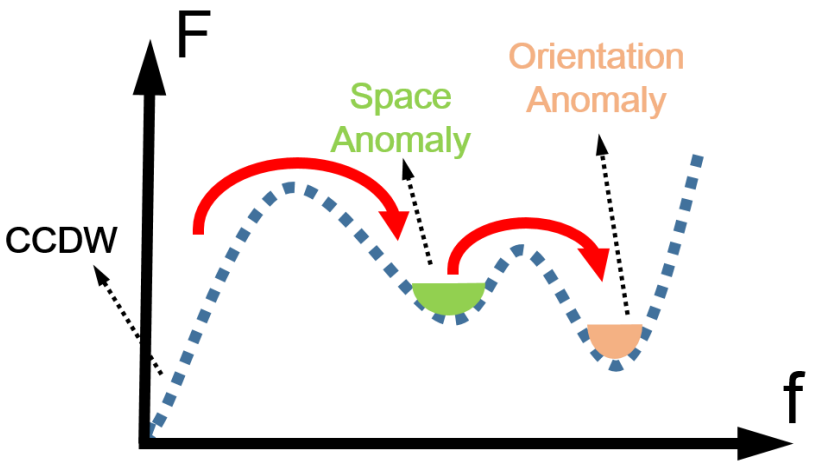

Fig. S4. CDW free energy schematic. (Color online) Schematic diagram of energy wells, illustrating the fluence-dependent switches of the space-anomaly H-CDW state and the orientation-anomaly H-CDW state.

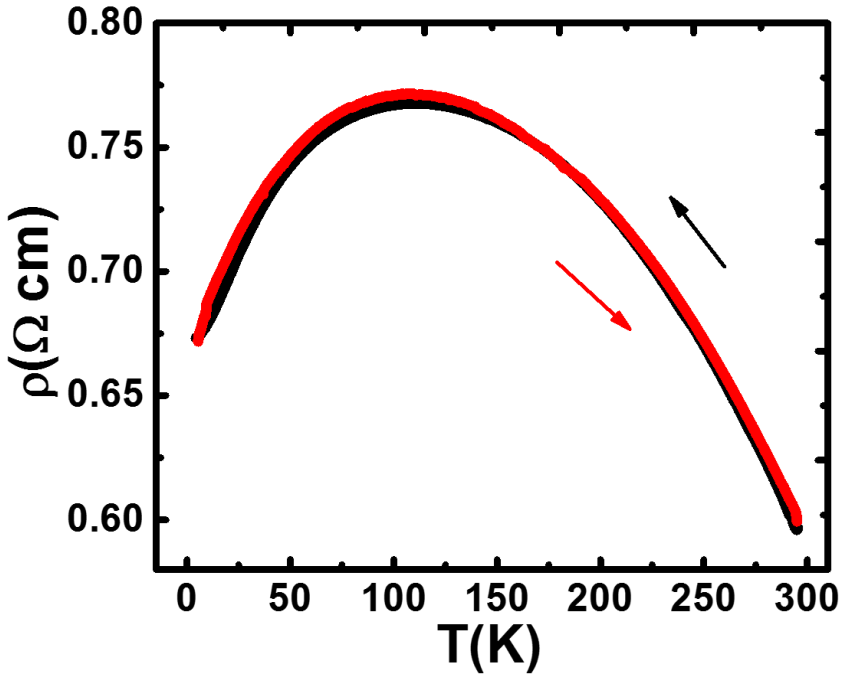

Fig. S5. Resistivity curve of 1T-TaSSe with photoexcitation. Temperature dependence of the resistivity on temperature cycling 1T-$TaS_{2-x}Se_x$ with x = 1. According to the electronic phase diagram (Fig. 1), there is no Mott state in x=1 sample. This sample performs superconductivity below ~ 3.6 K. We performed the ultrafast photoexcitation experiment in this sample at 4 K, 10 K and 20 K, but the resistivity has no change.

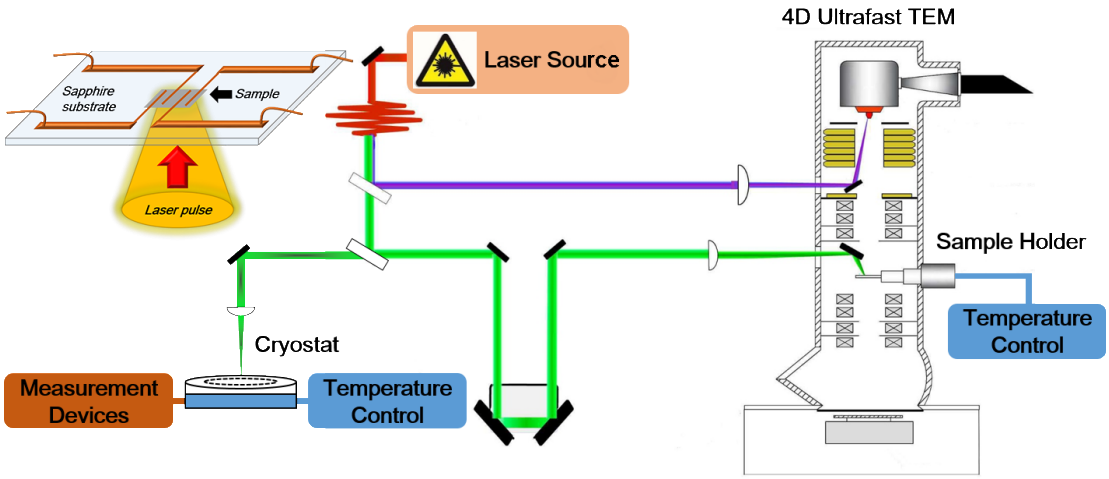

Fig. S6. Schematic diagram of the experimental setup. Schematic diagram of the experimental setup for in-situ photoexcitation measurements, as used inline with a 4D-ultrafast TEM (UTEM). The laser source can be shared for the measurements of physical properties and in-situ UTEM microstructure investigation. The inset displays the schematic of the experimental configuration of resistivity measurement; an exfoliated single sample on the sapphire substrate is used for resistivity measurements. Laser pulse illuminates the back of the sample.